ELSEVIER

Biophysical Chemistry 95 (2002) 183–193

Biophysical Chemistry

www.elsevier.com/locate/bpc

Hydrogen and deuterium in myoglobin as seen by a neutron structure determination at 1.5 Å resolution

Andreas Ostermann[a], Ichiro Tanaka[a], Niklas Engler[b], Nobuo Niimura[a], Fritz G. Parak[b,*]

[a]*Advanced Science Research Centre, JAERI, Tokai-Mura, lbaraki 319-1195, Japan*
[b]*Physik-Department E 17 der TUM, James Franck Str., 85747 Garching, Germany*

Received 7 June 2001; accepted 4 September 2001

Abstract

From the first days of protein neutron structure determination sperm whale myoglobin was an object under investigation [Nature 224 (1969) 143, J. Mol. Biol. 220 (1991) 381]. Nevertheless myoglobin is still of interest [Proc. Natl. Acad. Sci. USA 97 (2000) 3872]. The feasibility of the monochromatic neutron diffractometer BIX-3 at the JRR-3M reactor at the JAERI [J. Phys. Chem. Solids 60 (1999) 1623], to collect high-resolution diffraction data in a relatively short time stimulated us to repeat the structural determination of myoglobin. The structure of metmyoglobin has been determined up to a resolution of 1.5 Å. The hydrogen atoms were replaced in part, by deuterium soaking the crystals for more than 10 years in D_2O. A refinement of all atoms has been performed including the refinement of individual mean square displacements and occupancies of the exchangeable protons in backbone hydrogen bonds. A method is described to show clear negative scattering densities of the H atoms. Water molecules within the protein and on the molecule surface are shown. The exchangeability of H atoms is correlated with structural distribution and flexibility.

Keywords: Partial deuteration; Protein dynamics; Mean square displacement; Xenon hole

1. Introduction

Life depends on water. Water constitutes the main part of the human body. Most of the biochemical processes in cells need a water environment. Proteins lose their function if they become dry. All these facts show that the study of the interaction of water with biomolecules is of great interest. Moreover, biomolecules are often stabilized by hydrogen bonds. This internal network as it occurs for instance in α-helices, β-sheets or hairpin loops is in competition with hydrogen bonds of the residues and the water. Hydrogen atoms play an important role in biology. Their part in the structure and dynamics of biomolecules is an important field of research. Here, neutron scattering experiments are of exceptional value [1,2]. The progresses in the instrumentation of facilities for protein structure determination by neutrons [5–7] leads to an increasing number of solved structures. It also allows an improvement in resolution.

*Corresponding author. Tel.: +49-89-289-12551; fax: +49-89-289-12548.
E-mail address: fritz.parak@ph.tum.de (F.G. Parak).

0301-4622/02/$ - see front matter
PII: S0301-4622(01)00255-1

To reduce the incoherent background due to the scattering of hydrogen, it is common to exchange the buffer of the protein crystals by deuterated buffer. Moreover, this buffer exchange yields automatically an exchange of a number of protons of the protein. Another alternative is the perdeuteration of proteins by gene technology. Bacteria producing the proteins can be grown in heavy water and fed with a deuterated carbon source such as deuterated algae. Most scientists are convinced that this is the best way to obtain material for a neutron structure analysis of proteins.

In this contribution, we discuss a neutron structure analysis which was performed with a resolution of 1.5 Å. The crystals were soaked for several years in deuterated buffer. Here, we concentrate only on some selected topics. One aim is to show that partly deuterated proteins give complementary information compared with perdeuterated molecules.

2. Material and methods

Metmyoglobin from sperm whale was crystallized in a buffer of 50 mM KH_2PO_4, 2.9 M $(NH_4)_2SO_4$ at pH 6.8. Crystals of sufficient size were washed with the same buffer, which was subsequently exchanged by a buffer where all components had been deuterated to more than 95%. The crystals were allowed to exchange protons with deuterons in the solvent for more than 10 years. The sperm whale myoglobin crystal used in this study belongs to the space group $P2_1$ with unit cell constants: $a=64.53$ Å; $b=30.87$ Å; $c=34.87$ Å; and $\beta=105.7°$ and a crystal volume of 6.25 mm^3 ($2.5\times2.5\times1.0$ mm^3). For the measurement, the crystal was sealed in a quartz capillary. A sufficient amount of mother liquor was added to the bottom of the capillary to prevent the crystal from drying. Data were collected at room temperature at the monochromatic crystallography beam line BIX-3 at the JRR-3M reactor at the JAERI [4]. For data collection, the step scanning method was used, The data were collected in steps of $\Delta\varphi=0.3°$. The measurement time per frame was controlled by the monitor counts of the direct beam in front of the crystal and was approximately 30 min. After collecting 600 frames (180° rotation), the capillary was opened and the crystal rotated by approximately 90° within the capillary. Afterwards, additional 400 frames were measured under the same conditions. The data collection for a resolution range of 22–1.5 Å took 24 days.

A short estimation shows the advantage of the resolution of 1.5 Å. Myoglobin contains 1257 C, N an O atoms, 2 S and 1 Fe. In an X-ray refinement yielding three spatial coordinates together with the individual $\langle x^2\rangle$-values, for each atom we have 5040 parameters (without taking water molecules into account). At a resolution of 2 Å, we measured 8941 independent reflections of 9203 theoretically possible reflections. Thus, the number of parameters is still less than the number of reflections in the case of an X-ray structure analysis. This changes if we use neutrons. For the partly deuterated molecule, we have in addition, 997 H and 170 D atoms, which adds 4668 parameters, giving a total number of 9708 parameters. This means that an independent refinement of all parameters is no longer possible. The situation improves remarkably if we go to a resolution of 1.5 Å. Now there are 19 135 measured independent reflections of 21 493 theoretically possible reflections. Thus, a refinement of all atom coordinates, together with their mean square displacements can be performed.

The intensities of the reflections were integrated and scaled by the program DENZO and SCALEPACK [8]. The subsequent data reduction was performed by the CCP4 program TRUNCATE [9]. The refinement was done using the program X-PLOR versions 3.1 and 3.851 [10]. The protein topology file 'protein-allhdg.top' was used with small changes from the X-PLOR package. The protein parameter file 'protein.param' [11] from the CNS distribution was used after adding the missing parameters for the bonded hydrogen atoms. For the heme group, the X-PLOR files 'toph19x.pro' and 'toph19x.heme' were used after adding topology and parameter entries for the hydrogen atoms. The X-ray structure of metmyoglobin at 300 K determined up to 1.5 Å [12], was used as a starting model. The water coordinates from the X-ray model were removed and the positions of the non-exchangeable hydrogen atoms were generated due to stereochemical information from the topology file. This was fol-

Table 1
Data collection and refinement statistics

Data collection[a,b]							
Lower limit (Å)	Upper limit (Å)	No. refl.	No. unique	$\langle I\rangle/\langle\sigma(I)\rangle$	Compl. (%)	Multipl.	R_{merge} (%)
22.00	3.23	9143	2209	16.4	97.6	4.1	6.6
3.23	2.57	8334	2156	11.1	98.5	3.9	11.3
2.57	2.24	7057	2113	8.1	97.1	3.3	11.3
2.24	2.04	6140	2075	5.6	95.7	3.0	13.6
2.04	1.89	5468	2003	4.5	91.9	2.7	15.8
1.89	1.78	4859	1912	4.0	87.7	2.5	16.5
1.78	1.69	4344	1823	3.5	85.2	2.4	20.1
1.69	1.62	3995	1725	3.2	80.3	2.3	21.6
1.62	1.55	3518	1661	2.8	77.5	2.1	24.2
1.55	1.50	3041	1458	2.7	67.0	2.1	24.9
Overall		55 899	19 135	6.3	87.9	2.9	10.3

Refinement	
Resolution range (Å)	22.0–1.5
No. of reflections	19 135
Working set/test set	17 824/1311
$R_{cryt.}$ (%)	21.4
R_{free} (%)	24.7
r.m.s.d. bond length (Å)	0.007
r.m.s.d. bond angle (°)	1.2

[a] Space group = $P2_1$.

[b] Unit cell (Å, °): $a=64.53$; $b=30.87$; $c=34.87$ and $\beta=105.7$.

Data collection and refinement statistics. $R_{merge}=\sum_{hkl}\sum_i|I_i-\langle I\rangle|/\sum_{hkl}\sum_i\langle I\rangle$, where I_i is the intensity I for the ith measurement of the reflection with indices hkl and $\langle I\rangle$ is the mean of all measurements of the reflection I. $R_{cryst}=\sum_{hkl}|F_o(hkl)-F_c\times(hkl)|/\sum_{hkl}|F_o(hkl)|$, where $F_o(hkl)$ and $F_c(hkl)$ are the observed and calculated structure factor amplitudes for the reflection hkl. R_{free} is the crystallographic R-value calculated with the structure factor amplitudes of the test set, which is not involved in the refinement calculations.

lowed by an energy minimization for hydrogen atoms with rotational degrees of freedom (methyl-groups) without including the diffraction data. After a rigid body refinement and overall B-factor refinement, a positional refinement was performed with only the hydrogen atoms allowed to move. A F_o-F_c-map and $2F_o-Fc$-map was calculated. The positions of exchangeable hydrogen atoms were checked and were added to the model if a significant feature in the F_o-F_c- and $2F_o-F_c$-map was present. This was followed by a positional refinement and individual B-factor refinement (with special restraints, e.g. for methyl groups) with all atoms involved. Again F_o-F_c- and $2F_o-F_c$-maps were calculated and an inspection of exchangeable hydrogen positions and water positions was performed. This procedure was repeated until no interpretable significant density features could be observed in the F_o-F_c-map. The addition of solvent molecules to the model during this procedure was performed in steps of approximately 20 water molecules. The final model contains 62 water molecules of which 39 were modeled as D_2O molecules and one ND_4- and SO_4-molecule. All density map visualization and interpretation was done using the program 'O' [13]. A compilation of the statistical values for the data reduction and structure refinement is shown in Table 1.

As expected, the amide hydrogen atoms of the protein backbone show a different degree of exchange. To investigate this quantitatively, an occupancy refinement for these hydrogen atoms has been carried out. For this purpose, both a hydrogen atom (^1H, scattering length = -0.374×10^{-12} cm) and a deuterium atom (^2H,

scattering length $= 0.667 \times 10^{-12}$ cm) were generated at the refined position of the amide hydrogen atom. Due to the strong coupling of the B-factor and the occupancy of an atom the B-value of the hydrogen atoms were set to the refined value of the bonded nitrogen atom. For the occupancy refinement no constraint for adding up the occupancies to 1.0 was used. Even without such a constraint, the added fractional occupancy averaged of all backbone amide groups yields a value of 1.09 with a S.D. of 0.125.

3. Results and discussion

3.1. An improved visibility of protons:

Hydrogen atoms (^{1}H) can be visualized in neutron density maps as negative features. As has been discussed already by Kossiakoff and Spencer [14], and more recently by Shu et al. [3], it is often difficult to visualize hydrogen atoms (^{1}H) in the map. Shu et al. [3] discussed the poor visibility of hydrogen atoms even in scattering density maps calculated from a model (F_c map). They consider the cancellation of positive and negative density in the map as the problem, which leads to lower negative scattering density at the position of the hydrogen atoms. As our data have been collected to higher resolution, we have taken up this problem again.

The appearance of a scattering density map strongly depends on the scattering density level which is contoured. For the following analysis and for a well-defined comparison, all maps that are shown here are on an absolute scale. This means that the mean scattering density has been added. The contour levels are the same for all maps, namely: -0.13 cm^{-12}/Å^3 for negative; and $+0.27$ cm^{-12}/Å^3 for a positive density. The ratio of the contour levels equals the ratio of the mean positive scattering length to the scattering length of hydrogen. The negative contour level equals -1.5σ for a $2F_o$–F_c map. To calculate the maps shown in Fig. 1, no experimental data have been used. Instead, the structure of myoglobin has been used to calculate F_c maps up to 1.5 Å resolution at the heme. In Fig. 1a, all atoms are included; in Fig. 1b hydrogen atoms are excluded from the model. The map calculated without hydrogen atoms nevertheless shows a negative density, which should not be the case in a map based on absolute scattering densities. While the positive density in Fig. 1a reproduces a physically meaningful picture similar to the electron density obtained by X-ray structure analysis, the negative scattering density looks rather strange. Negative density can be seen correctly at some positions where it has to be, for instance at methyl groups. However, there is a strong negative density at positions where it definitively should not be present, for instance in the centers of the pyrrole rings. This demonstrates that the negative densities present in Fig. 1b are artifacts of the Fourier transform which is truncated at 1.5 Å. As neutrons are scattered by the nuclei, the scattered intensity as a function of scattering angle is a constant times the Debye–Waller factor. In Fig. 2 we show the comparison between X-ray and neutron scattering for a C-atom and the influence of the B-factor in the case of 1.5 Å resolution ($2\sin\theta/\lambda = 0.67$ Å^{-1}). It is obvious that for a reasonable B-value, the truncation is more severe in the case of neutron scattering yielding larger Fourier artifacts. Fourier artifacts are negligible only in maps calculated with a B-factor set to 40 Å^2.

In the case of neutron scattering, the negative scattering density can give valuable information on proton positions. Artificial negative scattering density diminishes the value of the interpretation. We got rid of most of these artifacts by the following procedure. The Fourier transform is a linear operation, thus we can subtract the maps shown in Fig. 1a,b in real space. The result is shown in Fig. 1c. The artificial negative density at the heme has vanished. In addition, the density at the hydrogen atoms has increased. This comes from two factors; the Fourier artifacts are removed and the positive density is subtracted. Thus our correction solves also the problem of cancellation discussed by Shu et al. [3]. The better known part of the protein, the heavy atoms, is subtracted to reveal the unknown part, the hydrogen atoms more clearly.

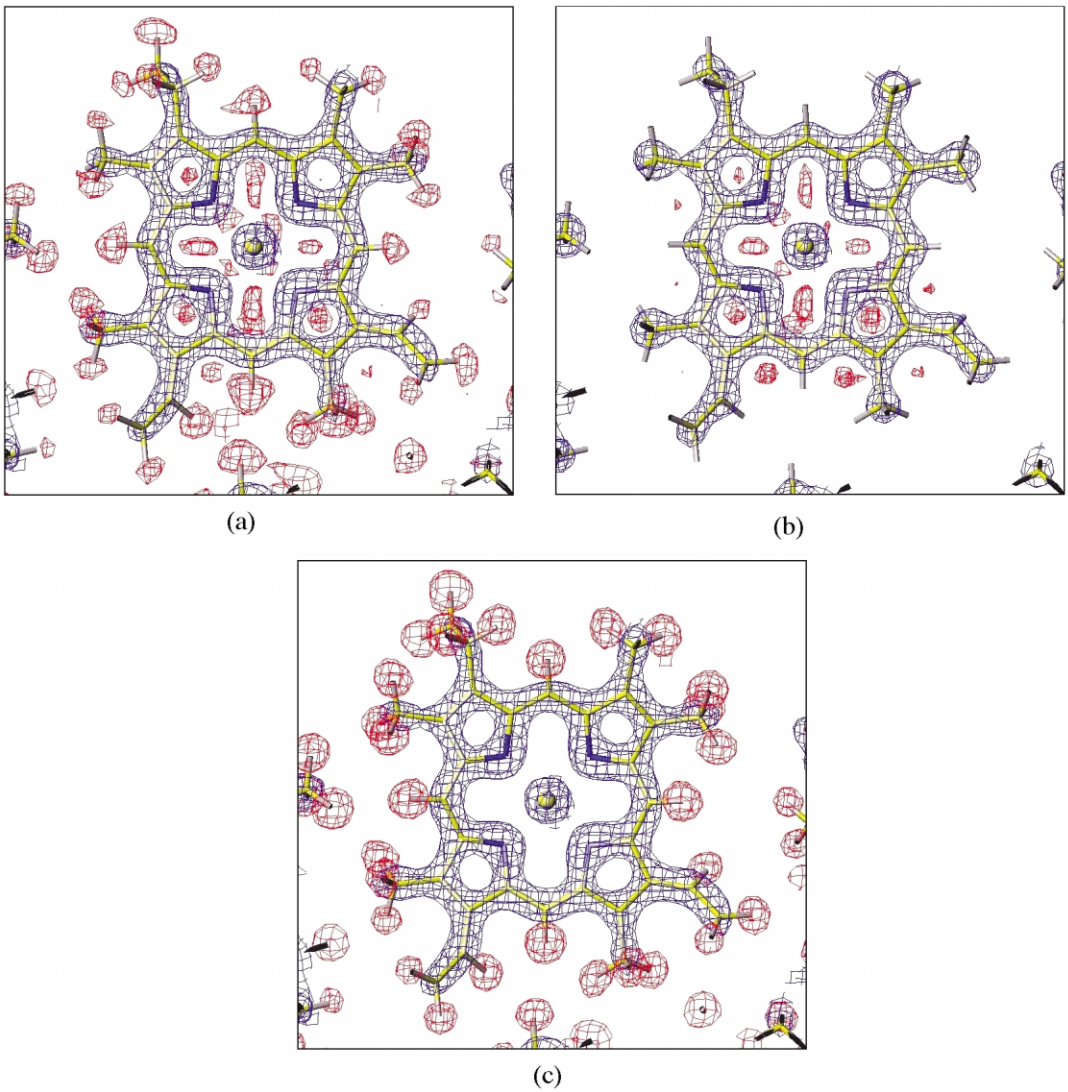

Fig. 1. Calculated neutron scattering density at the heme group (F_c maps) on absolute scales. (a) Positive scattering density in blue contoured at 0.27×10^{-12} cm/Å^3, and negative density in red contoured at -0.13×10^{-12} cm/Å^3. (b) The same as in (a), but calculated without hydrogen atoms. (c) The red map is the difference of the map shown in (a) and the map shown in (b), the blue map is the same as in (a).

Now we apply the same method to our experimental data. Note, that we again use absolute densities (by adding the calculated F_{000} reflection) and the contouring as in Fig. 1. Fig. 3 shows the obtained $2F_o-F_c$ maps. Fig. 3a gives the map without any correction. In Fig. 3b the map of Fig. 1b is subtracted. Again, most of the wrong negative density in the center of the heme group has been removed. The density at some hydrogen atoms has grown bigger, but at some there is still no negative density. Hydrogen atoms are often located in easily moving groups, e.g. methyl groups, which are therefore in some cases not visible at the displayed contour level. Comparing

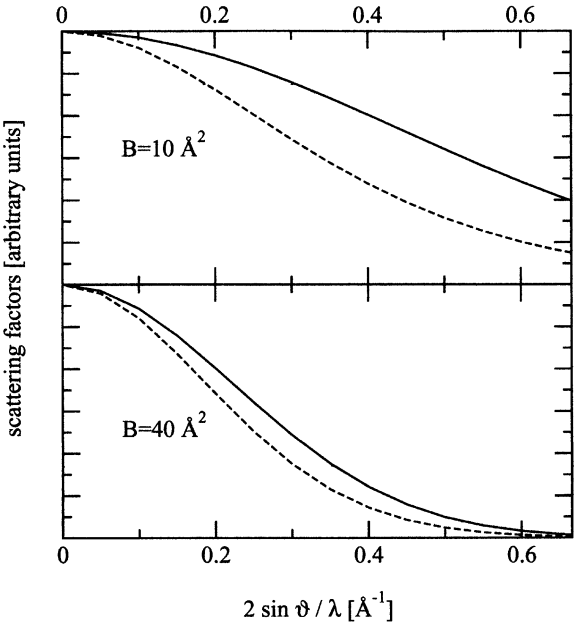

Fig. 2. Comparison of the scattering by an atom for X-rays (dashed line) and neutrons (straight line) as a function of the scattering angle. For a B-factor of: (a) 10; and (b) 40 Å^2.

Fig. 1c and Fig. 3b shows that the experimental data remain worse than the synthetic calculations. This is hardly surprising; the problem of true experimental noise cannot be overcome by our correction.

This correction procedure does not only help to visualize the hydrogen positions much better, but also helps to extract new information. To demonstrate this, we look at the methyl group marked by the arrow in Fig. 3b. Fig. 4a,b shows the methyl group as obtained by purely calculated maps before and after correction, respectively. Fig. 4c,d uses the experimental data and shows the $2F_o-F_c$ maps before and after subtraction of a calculated map, without hydrogen atoms. It is obvious that the model should be checked for the alternative position of the methyl group shown by the thin black lines in Fig. 4d. We want to remark that a $2F_o-Fc$ omit-map where the three hydrogen atoms have been omitted for the calculation of the F_c looks like Fig. 4c. As another example, we look at phenylalanine 43 as also shown by Shu et al. [3]. Fig. 5a,b give the $2F_o-F_c$ map before and after subtraction of the map without hydrogen atoms, respectively. The increase in visibility of the protons in the data reported here in comparison with the results reported by Shu et al. [3] is caused by the increase in resolution and the application of the correction procedure described above.

It should be emphasized that the described correction procedure has no influence on the refinement. However, it strongly improves the visibility of the hydrogen atoms and can therefore, be used to inspect the validity of the model as shown by the example in Fig. 4. All negative scattering density maps in this paper have been calculated by the described procedure.

3.2. The network of water molecules

In metmyoglobin, the sixth coordination of the heme iron is occupied by a water molecule. Both D-atoms are localized as shown in Fig. 6a. The D-atom making a hydrogen bond to the N_ε-atom of the distal histidine has an $\langle x^2\rangle$-value of 0.258 Å^2, while the O-atom is slightly better ordered with an $\langle x^2\rangle$-value of 0.163 Å^2. The second D-atom which forms no hydrogen bond, has an $\langle x^2\rangle$-value of 0.319 Å^2. The next water molecule is approximately 7 Å away and already on the surface of the molecule. Again, it is well defined with hydrogen bonds of 1.96 Å to one of the propionic acids of the heme and 2.84 Å to arginine 45. Inspecting the molecule surface close to arginine 45 on the upper right-hand-side of Fig. 6a, one finds a water network of four water molecules and one sulfate ion (compare Fig. 6b). This network lies just on the border between two myoglobin molecules in the crystal. In the contact region, the water molecules are well defined. With increasing distance from the surface of myoglobin, the waters become invisible due to high B-values.

3.3. The xenon holes

An essential function of myoglobin is the storage of an oxygen molecule. As discussed several times, the myoglobin model obtained by X-ray structure analysis shows no channel allowing the oxygen to enter the heme pocket. This problem has been the subject of several investigations. Of

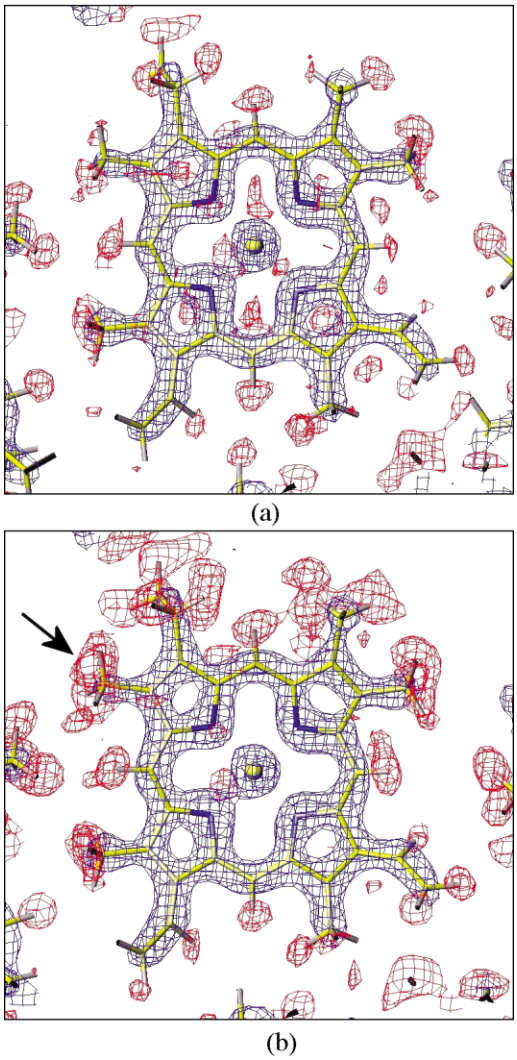

Fig. 3. (a) $2F_o–F_c$ maps without and (b) with correction (compare Fig. 1). For details see the text.

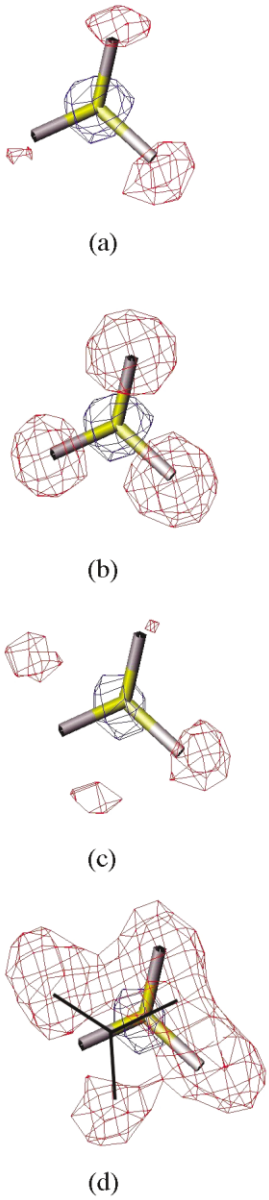

Fig. 4. The methyl group at the heme denoted by the arrow in Fig. 3b. (a) F_c map before correction. (b) Corrected F_c map. (c) $2F_o–F_c$ map before correction. (d) $2F_o–F_c$ map after correction.

great importance are the so-called Xe-holes (compare Fig. 7). It has been shown that at four places in myoglobin Xe-atoms can be disposed [15]. It is reasonable to say that the path of small molecules in or out of the protein moiety may go via these holes. In accordance with molecular dynamics simulations [16], it has been shown by X-ray structure analysis that hole no. 4 and 1 can be occupied by CO, if it is flashed off at low temperatures [17], [18], [19]. No CO has been found up to now in holes 2 and 3. We inspected the neutron scattering density map in the region of the Xe-holes in order to find water molecules. We could not see any water in holes 1, 2 and 4.

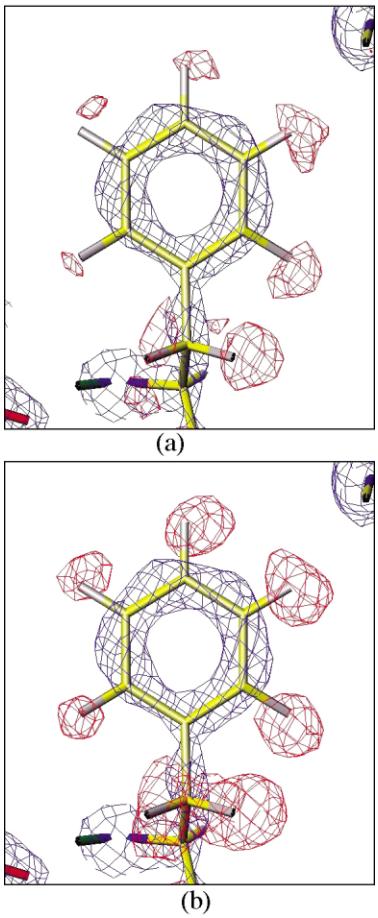

Fig. 5. $2F_o–F_c$ maps at phenylalanine 43. (a) Before and (b) after correction.

In hole 3, we found two water molecules fixed by hydrogen bonds. For one D_2O molecule, one D forms a hydrogen bond to a carbonyl oxygen and the other to a nitrogen atom of a histidine. By these two hydrogen bonds, the water is fixed and both deuterium atoms are visible. The second water molecule has no well-defined hydrogen bonds. The D-atoms are smeared out by disorder.

Here, we also want to show the influence of resolution. We have artificially reduced our data set to 3.0 Å. While the well defined water molecule is still clearly visible due to the large scattering length of D, the disordered one which is visible at 1.5 Å resolution disappears (compare Fig. 8b). Of course, this estimation is too optimistic since we use data of high quality. In a real experiment with only 3.0 Å resolution, the quality would be worse.

3.4. Protein dynamics

Information on protein dynamics can be obtained from the individual Debye–Waller factors of the atoms in the molecule which yield mean square displacements. The deuterium hydrogen exchange is another possibility to study protein dynamics. We want to combine both ways. Fig. 9a shows the mean square displacements of the backbone atoms of myoglobin as a function of residue number. All $\langle x^2 \rangle$-values are averages over

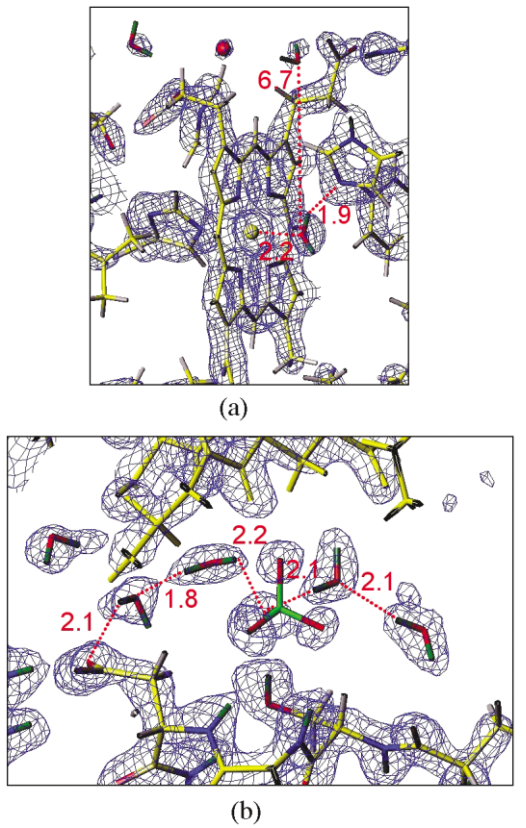

Fig. 6. (a) Positive scattering density in the heme region. The hydrogen bond distances and the distance (in Å) to the water nearest to the ligating water are shown. (b) Network of water molecules at the crystal contact to the next protein molecule. The density is contoured at 1.5σ. Note the SO_4^{2-} ion in the center of the figure.

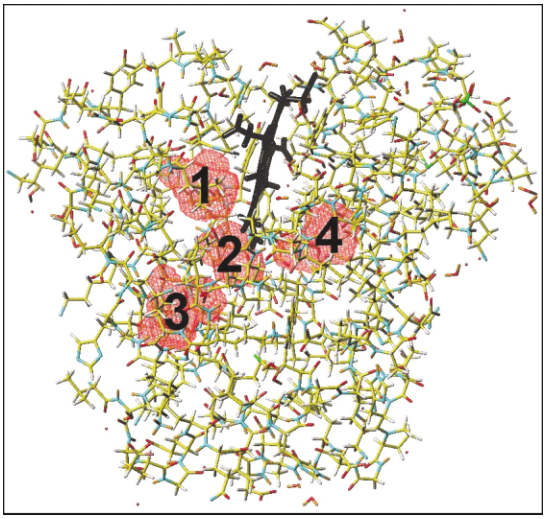

Fig. 7. Xenon holes in myoglobin. Numbering convention after Tilton et al. [15]. The cavities were calculated with the program VOIDOO [21].

the backbone atoms N–C–C–O. We compare two structure determinations performed on two crystals from the same batch. One structure was determined by X-ray scattering (1.5 Å resolution), one by neutron scattering. The absolute $\langle x^2\rangle$-values obtained from the neutron data are smaller than those obtained from the X-ray data. For a first view we normalized the neutron results to the X-ray data by:

$$\langle x^2\rangle_{n,\mathrm{norm}} = a\langle x^2\rangle_{n,\mathrm{exp}} + b. \quad (1)$$

A least squares fit of Eq. (1) to the $\langle x^2\rangle$-values obtained by X-ray structure analysis yielded $a = 1.21$ and $b = 0.044$ Å^2. The result is shown in Fig. 9a. It is obvious that both measurements give very similar results. Disorder, which comes at least in part, from dynamical effects, is seen at the same residues by neutrons and X-rays. There remains the question of the physical meaning of the parameters a and b. The parameter a is close to one; fixing a to 1.0 yields $b = 0.067$ Å^2, with only a slightly higher χ^2. Hence, the parameter a needs no discussion. An agreement of X-ray and neutron results could be obtained by multiplying the neutron amplitudes with $\exp[+8\pi^2 b\sin^2\theta/\lambda^2]$. Therefore, a possible explanation is a systematic overcorrection of the background in the case of neutron data. Weak reflections could become systematically too strong. However, at the present state we cannot rule out other effects.

It is well known that hydrogen atoms bound to the nitrogen of the peptide bond can be replaced by deuterium from D_2O. Therefore, the finding of

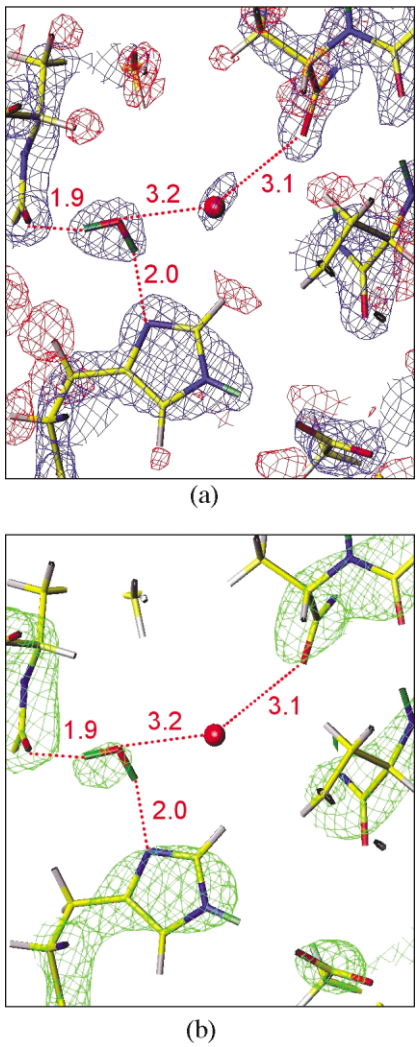

Fig. 8. Water molecules in the xenon-hole 3 (distances in Å). (a) Positive scattering density in blue, corrected negative scattering density in red. All reflections from 22–1.5 Å were used to calculate the map. Contour levels are 1.5 and -1.5σ, respectively. (b) Positive scattering density in green; only reflections from 22-3 Å were used to calculate the map. Contour level 1.5σ.

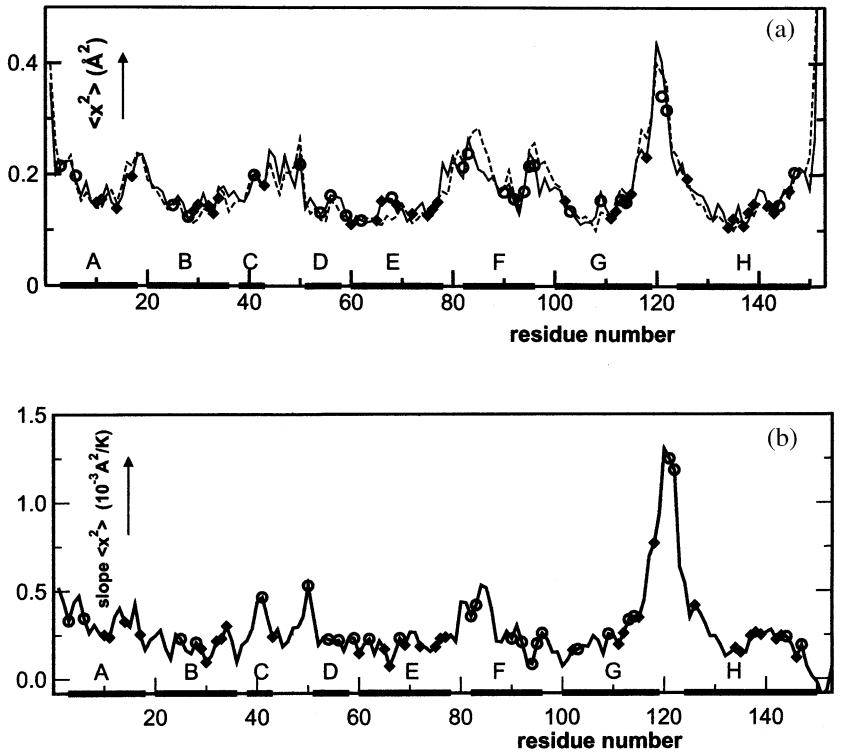

Fig. 9. (a) Mean square displacement, $\langle x^2 \rangle$, for the residues as a function of the residue number. Averages over the main chain atoms are shown. Dashed line: X-ray results; solid line: neutron results, the absolute values are normalized to the X-ray results; positions where more than 90% protons have exchanged to deuterons are marked by open circles, protons exchanged by less than 50% are marked by diamonds. (b) Slope of the linear temperature dependence of the mean squared displacement of the residues as function of the residue number (from X-ray data [12]) and the positions of the easily exchangeable and hardly exchangeable protons marked as in (a).

a N–D amide group proves that heavy water has been able to diffuse to the position of this group within the protein moiety. Even more than 10 years soaking of the crystals in deuterated buffer did not completely replace all N-bound hydrogen atoms. In Fig. 9 we marked all hydrogen atoms, which are exchanged by less than 50%. Their positions coincide with the position of residues with small $\langle x^2 \rangle$-values. Here, the myoglobin molecule is so well ordered that the diffusion of the water molecules is strongly restricted in these regions. Crystal structure analysis cannot differentiate $\langle x^2 \rangle$-values caused by dynamics or caused by static disorder. Dynamic effects depend on temperature. In myoglobin, the temperature dependence of the $\langle x^2 \rangle$-values is available in a large temperature interval [20,12]. In Fig. 9b the change of the $\langle x^2 \rangle$-values with temperature is plotted as function of the residue number. Again, the positions of less exchangeable hydrogen atoms are marked. They coincide with positions where the mean square displacements have only a rather weak temperature dependence. These regions are the most rigid parts of the molecule.

4. Conclusions

Protein structure determination by neutron scattering is a valuable tool for the determination of the hydrogen positions in the molecule and to study the hydration shell. Good resolution to typically 1.5 Å improves the accuracy drastically.

Perdeuteration of proteins makes experiments easier. It improves the quality of data significantly. However, we show here that also with partly deuterated proteins, a very good quality of data can be obtained yielding some complementary information. Partial deuteration by soaking crystals with deuterated buffer allows the differentiation between H and D atoms. If one gets rid of the Fourier artifacts as described above, a negative scattering density map clearly shows the positions of H-atoms and becomes very useful for the interpretation of the results.

References

[1] B.P. Schoenborn, Neutron diffraction analysis of myoglobin, Nature 224 (1969) 143–146.

[2] X. Cheng, B.P. Schoenborn, Neutron diffraction study of carbonmonoxy-myoglobin, J. Mol. Biol. 220 (1991) 381–399.

[3] F. Shu, V. Ramakrishnan, B.P. Schoenborn, Enhanced visibility of hydrogen atoms by neutron crystallography on fully deuterated myoglobin, Proc. Natl. Acad. Sci. USA 97 (2000) 3872–3877.

[4] I. Tanaka, K. Kurihara, Y. Haga, et al., An upgraded neutron diffractometer (BIX-I_M) for macromolecules with a neutron imaging plate, J. Phys. Chem. Solids 60 (1999) 1623–1626.

[5] N. Niimura, Y. Minezaki, T. Nonaka, et al., Neutron Laue diffractometry with an imaging plate provides an effective data collection regime for neutron protein crystallography, Nat. Struct. Biol. 4 (1997) 909–914.

[6] C. Bon, M.S. Lehmann, C. Wilkinson, Quasi-Laue neutron-diffraction study of the water arrangement in crystals of triclinic hen egg-white lysozyme, Acta Cryst. D 55 (1999) 978–987.

[7] J. Habash, J. Raftery, R. Nuttall, et al., Direct determination of the positions of the deuterium atoms of the bound water in concanavalin A by neutron Laue crystallography, Acta Cryst. D 56 (2000) 541–550.

[8] Z. Otwinowsky, W. Minor, Processing of X-ray diffraction data collected in oscillation mode, Methods Enzymol. 276 (1997) 307–326.

[9] S. Bailey, The CCP4 suite: programs for protein crystallography, Acta Cryst. D 50 (1994) 760–763.

[10] A.T. Brünger, X-PLOR Version 3.1, Yale University Press, New Haven, 1992.

[11] R.A. Engh, R. Huber, Accurate bond and angle parameters for X-ray protein structure refinement, Acta Cryst. A 47 (1991) 392–400.

[12] F.G. Parak, A. Ostermann, A. Gassmann, et al., Biomolecules: Fluctuations and Relaxations, in: H. Frauenfelder, G. Hummer, R. Garcia (Eds.), Biological Physics: Third International Symposium, American Institute of Physics, 1999, pp. 117–127.

[13] A. Jones, J.Y. Zou, S.W. Couran, M. Kjeldgaard, Improved methods for building protein models in electron density maps and the location of errors in these models, Acta Cryst. A 47 (1991) 110–119.

[14] A.A. Kossiakoff, S.A. Spencer, Direct determination of the protonation states of aspartic acid-102 and histidine-57 in the tetrahedral intermediate of the serine proteases: neutron structure of trypsin, Biochemistry 20 (1981) 6462–6474.

[15] R.F. Tilton, I.D. Kuntz, G.A. Petsko, Cavities in proteins: structure of a metmyoglobin–xenon complex solved to 1.9 Å, Biochemistry 23 (1984) 2849–2857.

[16] R. Elber, M. Karplus, Enhanced sampling in molecular-dynamics: use of the time-dependent Hartree approximation for a simulation of carbon-monoxide diffusion through myoglobin, J. Am. Chem. Soc. 112 (1990) 9161–9175.

[17] M. Brunori, B. Vallone, F. Cutruzzola, et al., The role of cavities in protein dynamics: crystal structure of a photolytic intermediate of a mutant myoglobin, Proc. Natl. Acad. Sci. USA 97 (2000) 2058–2063.

[18] K. Chu, J. Vojtchovsky, B.H. McMahon, R.M. Sweet, J. Berendzen, I. Schlichting, Structure of a ligand-binding intermediate in wild-type carbonmonoxy myoglobin, Nature 403 (2000) 921–923.

[19] A. Ostermann, R. Waschipky, F.G. Parak, G.U. Nienhaus, Ligand binding and conformational motions in myoglobin, Nature 404 (2000) 205–208.

[20] F. Parak, H. Hartmann, K.D. Aumann, et al., Low temperature X-ray investigation of structural distributions in myoglobin, Eur. Biophys. J. 15 (1987) 237–249.

[21] G.J. Kleywegt, T.A. Jones, Detection, delineation, measurement and display of cavities in macromolecular structures, Acta Cryst. D 50 (1994) 178–185.